Low-energy $K^- p \to \Lambda\eta$ reaction and the negative parity Λ resonances

Li-Ye Xiao and Xian-Hui Zhong[*]

Department of Physics, Hunan Normal University, and Key Laboratory of Low-Dimensional Quantum Structures
and Quantum Control of Ministry of Education, Changsha 410081, China

The reaction $K^- p \to \Lambda\eta$ at low energies is studied with a chiral quark model approach. Good descriptions of the existing experimental data are obtained. It is found that $\Lambda(1670)$ dominates the reaction around threshold. Furthermore, u- and t-channel backgrounds play crucial roles in this reaction as well. The contributions from the D-wave state $\Lambda(1690)$ are negligibly small for its tiny coupling to $\eta\Lambda$. To understand the strong coupling properties of the low-lying negative parity Λ resonances extracted from the $\bar{K}N$ scattering, we further study their strong decays. It is found that these resonances are most likely mixed states between different configurations. Considering these low-lying negative parity Λ resonances as mixed three-quark states, we can reasonably understand both their strong decay properties from Particle Data Group and their strong coupling properties extracted from the $\bar{K}N$ scattering. As a byproduct, we also predict the strong decay properties of the missing D-wave state $|\Lambda \frac{3}{2}^-\rangle_3$ with a mass of $\sim$1.8 GeV. We suggest our experimental colleagues search it in the $\Sigma(1385)\pi$ and $\Sigma\pi$ channels.

I. INTRODUCTION

Our knowledge about Λ resonances is much poorer than that of nucleon resonances [1]. Even for the well-established low-lying negative parity states, such as $\Lambda(1405)S_{01}$, $\Lambda(1520)D_{03}$, and $\Lambda(1670)S_{01}$, their properties are still controversial [2]. Up to now we cannot clarify whether these states are excited three-quark states, dynamically generated resonances, three-quark states containing multiquark components, or the other explanations, although there are extensive discussions about their natures [3–55].

Recently, we systematically studied the reactions $K^- p \to \Sigma^0 \pi^0, \Lambda\pi^0, \bar{K}^0 n$ in a chiral quark model approach [56]. Obvious roles of the low-lying negative parity states, $\Lambda(1405)$, $\Lambda(1520)$, and $\Lambda(1670)$, are found in the $K^- p \to \Sigma^0 \pi^0, \bar{K}^0 n$ reactions, where we have extracted their strong coupling properties. For example, we found that $\Lambda(1670)$ should have a very weak coupling to $\bar{K}N$, while $\Lambda(1520)$ needs a strong coupling to $\bar{K}N$, which cannot be well explained with the symmetry constituent quark model in the SU(6) $\otimes$ O(3) limit [56].

To obtain more strong coupling properties and better understandings of these low-lying Λ resonances, in this work, we continue to study another important $\bar{K}N$ reaction $K^- p \to \Lambda\eta$. This reaction provides us a very clear place to study the low-lying Λ resonances, because only the Λ resonances contribute here owing to the isospin selection rule. Especially the poorly known strong coupling of $\Lambda(1670)$ to $\eta\Lambda$ might be reliably obtained from the $K^- p \to \Lambda\eta$, for this reaction at threshold is dominated by formation of the $\Lambda(1670)$ [57]. Recently, the new data of the $K^- p \to \Lambda\eta$ reaction from Crystal Ball Collaboration [57] were analyzed with an effective Lagrangian model by Liu and Xie [51,52]. They might find some evidence of a exotic D-wave resonance

with mass $M \simeq 1669$ MeV and width $\Gamma \simeq 1.5$ MeV in the reaction, which is discussed in present work as well.

Furthermore, to understand the natures of these strong coupling properties extracted from the $\bar{K}N$ scattering, we further carry out a systematical study of the strong decays of the low-lying negative parity Λ resonances in the chiral quark model approach as well. Combing the strong coupling properties extracted from the $\bar{K}N$ scattering with the strong decay properties from the Particle Data Group (PDG) [1], we expect to obtain more reliable understandings of the natures for these low-lying negative parity Λ resonances.

This work is organized as follows. In Sec. II, the model is reviewed. Then, the numerical results are presented and discussed in Sec. III. Finally, a summary is given in Sec. IV.

II. FRAMEWORK

In this work, we study the $K^- p \to \Lambda\eta$ reaction in a chiral quark model. This model has been well developed and widely applied to meson photoproduction reactions [58–66]. Its recent extension to describe the πN [67] and $\bar{K}N$ [42,56] reactions also turns out to be successful and inspiring.

In the calculations, we consider three basic Feynman diagrams, i.e., s, u, and t channels at the tree level. The reaction amplitude is expressed as

$$\mathcal{M} = \mathcal{M}_s + \mathcal{M}_u + \mathcal{M}_t, \tag{1}$$

where the s- and u-channel reaction amplitudes $\mathcal{M}_s$ and $\mathcal{M}_u$ are given by

$$\mathcal{M}_s = \sum_j \langle N_f | H_m^f | N_j \rangle \langle N_j | \frac{1}{E_i + \omega_i - E_j} H_m^i | N_i \rangle, \tag{2}$$

$$\mathcal{M}_u = \sum_j \langle N_f | H_m^i \frac{1}{E_i - \omega_f - E_j} | N_j \rangle \langle N_j H_m^f | N_i \rangle. \tag{3}$$

In the above equations, H_m stands for the quark-meson coupling, which might be described by the effective chiral

_____
*zhongxh@hunnu.edu.cn

Lagrangian [58,59]

$$H_m = \sum_j \frac{1}{f_m} \overline{\psi}_j \gamma_u^j \gamma_5^j \psi_j \vec{\tau} \cdot \partial^u \vec{\phi}_m, \qquad (4)$$

where ψ_j represents the jth quark field in a baryon and f_m is the meson's decay constant. The pseudoscalar meson octet ϕ_m is written as

$$\phi_m = \begin{pmatrix} \frac{1}{\sqrt{2}}\pi^0 + \frac{1}{\sqrt{6}}\eta & \pi^+ & K^+ \\ \pi^- & -\frac{1}{\sqrt{2}}\pi^0 + \frac{1}{\sqrt{6}}\eta & K^0 \\ K^- & \bar{K}^0 & -\sqrt{\frac{2}{3}}\eta \end{pmatrix}. \qquad (5)$$

In Eqs. (2) and (3), ω_i and ω_f are the energies of the incoming and outgoing mesons, respectively. $|N_i\rangle$, $|N_j\rangle$, and $|N_f\rangle$ stand for the initial, intermediate, and final states, respectively, and their corresponding energies are E_i, E_j, and E_f, which are the eigenvalues of the nonrelativistic Hamiltonian of constituent quark model $\hat{H}$ [3–5].

The resonance transition amplitudes of the s channel can be generally expressed as [67]

$$\mathcal{M}_R^s = \frac{2M_R}{s - M_R^2 + i M_R \Gamma_R} \mathcal{O}_R e^{-(\mathbf{k}^2 + \mathbf{q}^2)/(6\alpha^2)}, \qquad (6)$$

where M_R and Γ_R stand for the mass and width of the resonance, respectively. The Mandelstam variable s is defined as $s \equiv (P_i + k)^2$. The single-resonance-excitation amplitude, $\mathcal{O}_R$, can be obtained by the relation [56]

$$\mathcal{O}(n, l, J) = \sum_R \mathcal{O}_R(n, l, J) = \sum_R g_R \mathcal{O}(n, l, J), \qquad (7)$$

where g_R stands for the relative strength of a single-resonance in the partial amplitude $\mathcal{O}(n, l, J)$. The g_R factors are determined by the structure of each resonance and their couplings to the meson and baryon. The partial amplitudes, $\mathcal{O}(n, l, J)$, up to the $n = 2$ shell have been derived in our previous work [56], where the details can be found. For example, the important partial amplitude for the S waves is given by [56]

$$\mathcal{O}_1(S) = \left(g_{s1} - \frac{1}{2}g_{s2}\right)\left(|\mathbf{A}_{\text{out}}| \cdot |\mathbf{A}_{\text{in}}| \frac{|\mathbf{k}||\mathbf{q}|}{9\alpha^2} + \frac{\omega_i}{6\mu_q}\mathbf{A}_{\text{out}} \cdot \mathbf{q}\right.$$
$$\left. + \frac{\omega_f}{6\mu_q}\mathbf{A}_{\text{in}} \cdot \mathbf{k} + \frac{\omega_i \omega_f}{4\mu_q \mu_q}\alpha^2\right), \qquad (8)$$

where $\mathbf{k}$ and $\mathbf{q}$ stand for the three-momenta of the incoming and outgoing mesons, respectively, and α is the harmonic oscillator parameter. The reduced mass μ_q at the quark level is defined by $1/\mu_q = 1/m_q^i + 1/m_q^f$, where m_q^i and m_q^f correspond to the initial and final quark masses, respectively. $\mathbf{A}_{\text{in}}$ and $\mathbf{A}_{\text{out}}$ are the same variables defined in Ref. [56]. The g factors in the partial amplitudes, such as g_{s1} and g_{s2}, have been defined in Ref. [56] as well. These g factors can be derived in the SU(6) ⊗ O(3) symmetry limit. In Table I, we have listed the g factors for the reaction $K^- p \rightarrow \Lambda \eta$.

The transition amplitudes of the u channel are given by [42,67]

$$\mathcal{M}_n^u = -\frac{2M_n}{u - M_n^2} \mathcal{O}_n e^{-(\mathbf{k}^2 + \mathbf{q}^2)/(6\alpha^2)}. \qquad (9)$$

TABLE I. The g factors appearing in the s-, u-, and t-channel amplitudes of the $K^- p \rightarrow \Lambda \eta$ process obtained in in the SU(6) ⊗ O(3) symmetry limit. ϕ_p is the η-η' mixing angle defined in Refs. [68,69].

$g_{s1} = -\frac{\sqrt{6}}{6}\sin\phi_p$	$g_{v1} = -\frac{\sqrt{6}}{4}\sin\phi_p$
$g_{s1}^u = \frac{\sqrt{3}}{2}\cos\phi_p$	$g_{v1}^u = \frac{\sqrt{3}}{2}\cos\phi_p$
$g_t^s = \frac{\sqrt{6}}{2}$	$g_t^v = \frac{\sqrt{6}}{2}$

In Eq. (9), the amplitude $\mathcal{O}_n$ is determined by the structure of each resonance and their couplings to the meson and baryon, which has been derived in our previous work [56]. The Mandelstam variable u is defined as $u \equiv (P_i - q)^2$.

In the calculations, we consider the vector and scalar exchanges for the t-channel backgrounds. The vector meson-quark and scalar meson-quark couplings are given by

$$H_V = \bar{\psi}_j\left(a\gamma^v + \frac{b\sigma^{v\lambda}\partial_\lambda}{2m_q}\right)V_v \psi_j, \qquad (10)$$

$$H_S = g_{Sqq}\bar{\psi}_j \psi_j S, \qquad (11)$$

where V and S stand for the vector and scalar fields, respectively. The constants a, b, and g_{Sqq} are the vector, tensor, and scalar coupling constants, respectively. They are treated as free parameters in this work.

However, the VPP and SPP couplings (P stands for a pseudoscalar-meson) are adopted as

$$H_{VPP} = -iG_V \text{Tr}([\phi_m, \partial_\mu \phi_m]V^\mu), \qquad (12)$$

$$H_{SPP} = \frac{g_{SPP}}{2m_\pi}\partial_\mu \phi_m \partial^\mu \phi_m S, \qquad (13)$$

where G_V and g_{SPP} are the VPP and SPP coupling constants, respectively, to be determined by experimental data.

For the vector meson exchange, the t-channel amplitude in the quark model is written as [56]

$$\mathcal{M}_t^V = \mathcal{O}_V^t \frac{1}{t - M_V^2} e^{-(\mathbf{q} - \mathbf{k})^2/(6\alpha^2)}, \qquad (14)$$

where $e^{-(\mathbf{q}-\mathbf{k})^2/(6\alpha^2)}$ is a form factor deduced from the quark model, and M_V is the vector-meson mass. The amplitude $\mathcal{O}_V^t$ is given by [56]

$$\mathcal{O}_V^t = G_v a\big[g_t^s(\mathcal{H}_0 + \mathcal{H}_1 \mathbf{q} \cdot \mathbf{k}) + g_t^v \mathcal{H}_2 i\sigma \cdot (\mathbf{q} \times \mathbf{k})\big]$$
$$+ \text{tensor term}, \qquad (15)$$

where the factors g_t^s and g_t^v are defined by $g_t^s \equiv \langle N_f | \sum_{j=1}^3 I_j^{\text{ex}} | N_i \rangle$ and $g_t^v \equiv \langle N_f | \sum_{j=1}^3 \sigma_j I_j^{\text{ex}} | N_i \rangle$, respectively, where I_j^{ex} is the isospin operator of exchanged meson. These factors can be deduced from the quark model.

For the scalar meson exchange, the t-channel amplitude in the quark model is given by [56]

$$\mathcal{M}_t^S = \mathcal{O}_S^t \frac{1}{t - M_S^2} e^{-(\mathbf{q} - \mathbf{k})^2/(6\alpha^2)}, \qquad (16)$$

where M_S is the scalar-meson mass, and the $\mathcal{O}_S^t$ is written as [56]

$$\mathcal{O}_S^t \simeq \frac{g_{SPP}g_{Sqq}}{2m_\pi}(\omega_i \omega_f - \mathbf{q} \cdot \mathbf{k})$$
$$\times \big[g_t^s(\mathcal{A}_0 + \mathcal{A}_1 \mathbf{q} \cdot \mathbf{k})g_t^v \mathcal{A}_2 i\sigma \cdot (\mathbf{q} \times \mathbf{k})\big]. \qquad (17)$$

In Eqs. (15) and (17), the variables $\mathcal{H}_i$ and $\mathcal{A}_i$ ($i = 0, 1, 2$) are the same definitions as in Ref. [56].

In this work, we consider the K^* and κ exchanges in the $K^- p \to \Lambda \eta$ process. The factors g_t^s and g_t^v derived from the quark model have been listed in Table I as well.

III. RESULT AND ANALYSIS

A. Parameters

With the transition amplitudes derived within the quark model, the differential cross section can be calculated by [56]

$$\frac{d\sigma}{d\Omega} = \frac{(E_i + M_i)(E_f + M_f)}{64\pi^2 s (2M_i)(2M_f)} \frac{|\mathbf{q}|}{|\mathbf{k}|} \frac{M_N^2}{2}$$
$$\times \sum_{\lambda_i, \lambda_f} \left| \left[\frac{\delta_{m_i}}{f_{m_i}} \frac{\delta_{m_f}}{f_{m_f}} (\mathcal{M}_s + \mathcal{M}_u) + \mathcal{M}_t \right]_{\lambda_f, \lambda_i} \right|^2, \quad (18)$$

where $\lambda_i = \pm 1/2$ and $\lambda_f = \pm 1/2$ are the helicities of the initial- and final-state Λ baryons, respectively. f_{m_i} and f_{m_f} are the initial and final meson decay constants, respectively. $\delta_{m_i} \delta_{m_f}$ is a global parameter accounting for the flavor symmetry-breaking effects arising from the quark-meson couplings, which will be determined by experimental data.

In the calculation, the universal value of harmonic oscillator parameter $\alpha = 0.4$ GeV is adopted. The masses of the u, d, and s constituent quarks are set as $m_u = m_d = 330$ MeV and $m_s = 450$ MeV, respectively. The decay constants for η and K are adopted as $f_\eta = f_K = 160$ MeV.

In present work, the resonance transition amplitude, $\mathcal{O}_R$, is derived in the SU(6) ⊗ O(3) symmetric quark model limit. In reality, owing to, e.g., spin-dependent forces in the quark-quark interaction, the symmetry of SU(6) ⊗ O(3) is generally broken. As a result, configuration mixing would occur [3–5,11], which would alter the value of the resonance transition amplitudes. Furthermore, the hadronic dressing effects of the vertexes might bring uncertainties to the resonance transition amplitudes as well [40,70,71]. To take into account the symmetry-breaking and hadronic dressing effects, a set of coupling strength parameters, C_R, should be introduced for each resonance amplitude,

$$\mathcal{O}_R \to C_R \mathcal{O}_R, \quad (19)$$

where C_R should be determined by fitting the experimental observation. The determined values of C_R for the $K^- p \to \Lambda \eta$ process have been listed in Table II. These strength parameters C_R for the main resonances are further discussed in Sec. III D.

In the t channel, there are two parameters, $G_V a$ and $g_{SPP} g_{Sqq}$, which come from K^* and κ exchanges, respectively. By fitting the data, we obtain $G_V a \simeq 4.8$ and $g_{SPP} g_{Sqq} \simeq 105$, which are consistent with our previous determinations in Ref. [56].

TABLE III. The classification of Λ resonances in the quark model up to the $n = 2$ shell. The "?" denotes the resonances being unestablished. $l_{I,2J}$ is the PDG notation of baryons. N_6 and N_3 denote the SU(6) and SU(3) representations. L and S stand for the total orbital momentum and spin of a baryon, respectively.

$\lvert N_6, {}^{2S+1} N_3, n, L \rangle$	$l_{I,2J}$	$\lvert N_6, {}^{2S+1} N_3, n, L \rangle$	$l_{I,2J}$
$\lvert 56, {}^2 8, 0, 0 \rangle$	$P_{01}(1116)$	...	...
$\lvert 70, {}^2 1, 1, 1 \rangle$	$S_{01}(1405)$	$\lvert 56, {}^2 8, 2, 2 \rangle$	$P_{03}(?)$
	$D_{03}(1520)$		$F_{05}(?)$
$\lvert 70, {}^2 8, 1, 1 \rangle$	$S_{01}(1670)$	$\lvert 70, {}^2 1, 2, 2 \rangle$	$P_{03}(?)$
	$D_{03}(1690)$		$F_{05}(?)$
$\lvert 70, {}^4 8, 1, 1 \rangle$	$S_{01}(1800)$	$\lvert 70, {}^2 8, 2, 2 \rangle$	$P_{03}(?)$
	$D_{03}(?)$		$F_{05}(?)$
	$D_{05}(1830)$		
$\lvert 56, {}^2 8, 2, 0 \rangle$	$P_{01}(1600)$	$\lvert 70, {}^4 8, 2, 2 \rangle$	$P_{01}(?)$
$\lvert 70, {}^2 1, 2, 0 \rangle$	$P_{01}(1810)$		$P_{03}(?)$
$\lvert 70, {}^2 8, 2, 0 \rangle$	$P_{01}(?)$		$F_{05}(?)$
$\lvert 70, {}^4 8, 2, 0 \rangle$	$P_{03}(?)$		$F_{07}(?)$

In the u channel, the intermediate states are nucleon and nucleon resonances. One finds that the contributions from $n \geqslant 1$ shell are negligibly small and are insensitive to the degenerate masses for these shells. In present work, we take $M_1 = 1650$ MeV and $M_2 = 1750$ MeV for the degenerate masses of $n = 1$ and $n = 2$ shell nucleon resonances, respectively.

In the s channel of the $K^- p \to \Lambda \eta$ process, there are only the contributions from Λ resonances. The low-lying Λ resonances classified in the quark model up to the $n = 2$ shell are listed in Table III. From the table, we can see that in the $n = 0$ shell only the Λ pole contributes to the process, while in the $n = 1$ shell two S waves [i.e., $[70, {}^2 1]\Lambda(1405)S_{01}$, $[70, {}^2 8]\Lambda(1670)S_{01}$] and two D waves [i.e., $[70, {}^2 1]\Lambda(1520)D_{03}$, $[70, {}^2 8]\Lambda(1690)D_{03}$] contribute to the reaction. The excitations of $[70, {}^4 8]$ are forbidden for the Λ-selection rule [72]. In the calculations, the $n = 2$ shell Λ resonances in the s channel are treated as degeneration, and their degenerate mass and width are taken as $M = 1800$ MeV and $\Gamma = 100$ MeV, because in the low-energy region the contributions from the $n = 2$ shell are not significant.

By fitting the experimental data, we obtain their Breit-Wigner masses and widths, which are listed in Table IV. From the table, it is seen that the extracted resonances' parameters are compatible with the data from PDG [1].

TABLE II. The determined values for the parameters C_R, $\delta_{m_i} \delta_{m_f}$, and ϕ_P in the $K^- p \to \Lambda \eta$ scatting process.

Parameter	$C_{S_{01}(1405)}$	$C_{D_{03}(1520)}$	$C_{S_{01}(1670)}$	$C_{D_{03}(1690)}$	$\delta_{m_i} \delta_{m_f}$	ϕ_P
Value	1.17	1.18	34.70	38.58	1.24	$35°$

TABLE IV. Breit-Wigner masses M_R (MeV) and widths Γ_R (MeV) for the resonances in the s channel compared with the experimental data from PDG [1].

Resonance	M_R	Γ_R	M_R (PDG)	Γ_R (PDG)
$\Lambda(1405)S_{01}$	1405.0	53.4	$1405.0^{+1.3}_{-1.0}$	50 ± 2
$\Lambda(1520)D_{03}$	1519.5	15.6	1519.5 ± 1.0	15.6 ± 1.0
$\Lambda(1670)S_{01}$	1676.0	35.0	1670 ± 10	25–50
$\Lambda(1690)D_{03}$	1682.4	70.0	1690 ± 5	50–70
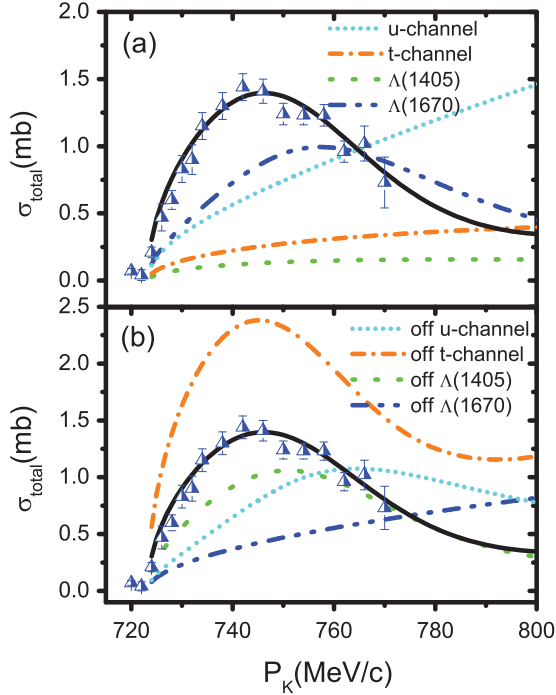
FIG. 1. (Color online) $K^- p \to \Lambda \eta$ total cross sections compared with the data [57]. The bold solid curves are for the full model calculations. In the top panel, exclusive cross sections for $\Lambda(1405)S_{01}$, $\Lambda(1670)S_{01}$, t channel, and u channel are indicated explicitly by the legends in the figures. In the bottom panel, the results by switching off the contributions of $\Lambda(1405)S_{01}$, $\Lambda(1670)S_{01}$, t channel, and u channel are indicated explicitly by the legends in the figures.

B. Total cross section

The total cross section as a function of the beam momentum is shown in Fig. 1, where we find that the observations can be well described within the chiral quark model.

It is found that $\Lambda(1670)S_{01}$ should play a dominant role in the reaction. $\Lambda(1670)S_{01}$ is responsible for the bump structure in the cross section around its threshold. To well describe the data, a large amplitude of $\Lambda(1670)S_{01}$ in the reaction is needed, which is about 34 times (i.e., $C_{S_{01}(1670)} = 34$) larger than that derived in the $SU(6) \otimes O(3)$ limit. In our previous work, we found $\Lambda(1670)S_{01}$ should have a weaker coupling to $\bar{K}N$ than that derived in the $SU(6) \otimes O(3)$ limit [56]; thus, $\Lambda(1670)S_{01}$ should have a much stronger coupling to $\eta\Lambda$ than that derived from the symmetry quark model. These phenomena might be explained by the configuration mixing between the S-wave states $\Lambda(1405)S_{01}$, $\Lambda(1670)S_{01}$, and $\Lambda(1800)S_{01}$, which are further studied in Sec. III D.

Furthermore, a sizable contribution from $\Lambda(1405)$ might be seen in the cross section. The total cross section around the peak is slightly underestimated without its contribution. It should be mentioned that because the $\Lambda(1405)S_{01}$ is far away from the $\eta\Lambda$ threshold, the information of $\Lambda(1405)S_{01}$ obtained from the $K^- p \to \Lambda \eta$ process might be unreliable.

No obvious contributions from the D-wave states, $\Lambda(1520)D_{03}$ and $\Lambda(1690)D_{03}$, are found in the reaction.

It should be emphasized that both u- and t-channel backgrounds play crucial roles in the reactions. Switching off their

contributions, the cross section changes significantly. The important roles of u- and/or t-channel backgrounds are also found in the other $\bar{K}N$ reactions $K^- p \to \Sigma^0 \pi^0$, $\Lambda \pi^0$, $\bar{K}^0 n$ [56].

C. Differential cross section

The differential cross sections (DCSs) compared with the data are shown in Fig. 2. From the figure, it is seen that the data in the low-energy region from threshold to $P_K = 770$ MeV/c can be reasonably described within our chiral quark model. However, it should be remarked that our theoretical results seem to slightly underestimate the DCS at both forward and backward angles in the beam momenta region of $P_K = 730$–742 MeV/c. Improved measurements in this beam momenta region are needed to clarify the discrepancies.

To explore the contribution of individual resonances and the u- and t-channel backgrounds to the DCS, we have shown the predictions by switching off one of their contributions in Fig. 2 as well. From the figure, the dominant roles of $\Lambda(1670)S_{01}$ and u- and t-channel backgrounds are significantly seen in the DCS. Switching off the contribution of $\Lambda(1670)S_{01}$, we find that the cross sections will be underestimated draftly. Without the u-channel contribution, the DCS will be significantly underestimated around the η production threshold. While switching off t-channel contribution, we can see that the DCS are strongly overestimated at both forward and backward angles. Furthermore, slight contributions of $\Lambda(1405)S_{01}$ might be seen in the DCS around the η production threshold, where $\Lambda(1405)S_{01}$ has a slight constructive interference with $\Lambda(1670)S_{01}$. However, $\Lambda(1405)S_{01}$ is not a crucial contributor in the reaction. We might not obtain any reliable information of $\Lambda(1405)S_{01}$ from the $K^- p \to \Lambda \eta$ process. Thus, the contribution of $\Lambda(1405)S_{01}$ are usually neglected in some studies at the hadron level [37,51,52].

From Fig. 2, it is seen that a bowl structure seems to appear in the data around the η production threshold. As we know, the bowl structures are the typical effects of the interferences between the S- and D-wave states. In this energy region, the bowl structures might be caused by the interferences between $\Lambda(1670)S_{01}$ and $\Lambda(1690)D_{03}$. Considering $\Lambda(1690)D_{03}$ as the conventional three-quark state classified in the constituent quark model, we cannot obtain a bowl structure in the DCS for the too-small contributions of $\Lambda(1690)D_{03}$ in the reaction. In Refs. [51,52], Liu and Xie had carefully studied these bowl structures appearing in the DCS, they need an exotic D-wave state $\Lambda(1669)$ with a very narrow width of $\Gamma \simeq 1.5$ MeV to reproduce the bowl structures. Finally, it should be pointed out that for the rather large uncertainties of the present data, we cannot confirm whether there are obvious bowl structures in the DCS or not. Thus, more accurate measurements are needed.

As a whole, $\Lambda(1670)S_{01}$ plays a dominant role in the reaction. $\Lambda(1670)S_{01}$ should have a much stronger coupling to $\eta\Lambda$, while having a weaker coupling to $\bar{K}N$ than that derived in the $SU(6) \otimes O(3)$ limit. The u- and t-channel backgrounds also play crucial roles in the reaction. Furthermore, slight contributions of $\Lambda(1405)S_{01}$ might be seen in the DCS around the η production threshold. It should be pointed out that for the large distance of $\Lambda(1405)S_{01}$ to the $\eta\Lambda$ threshold and the limitations of our model, the information
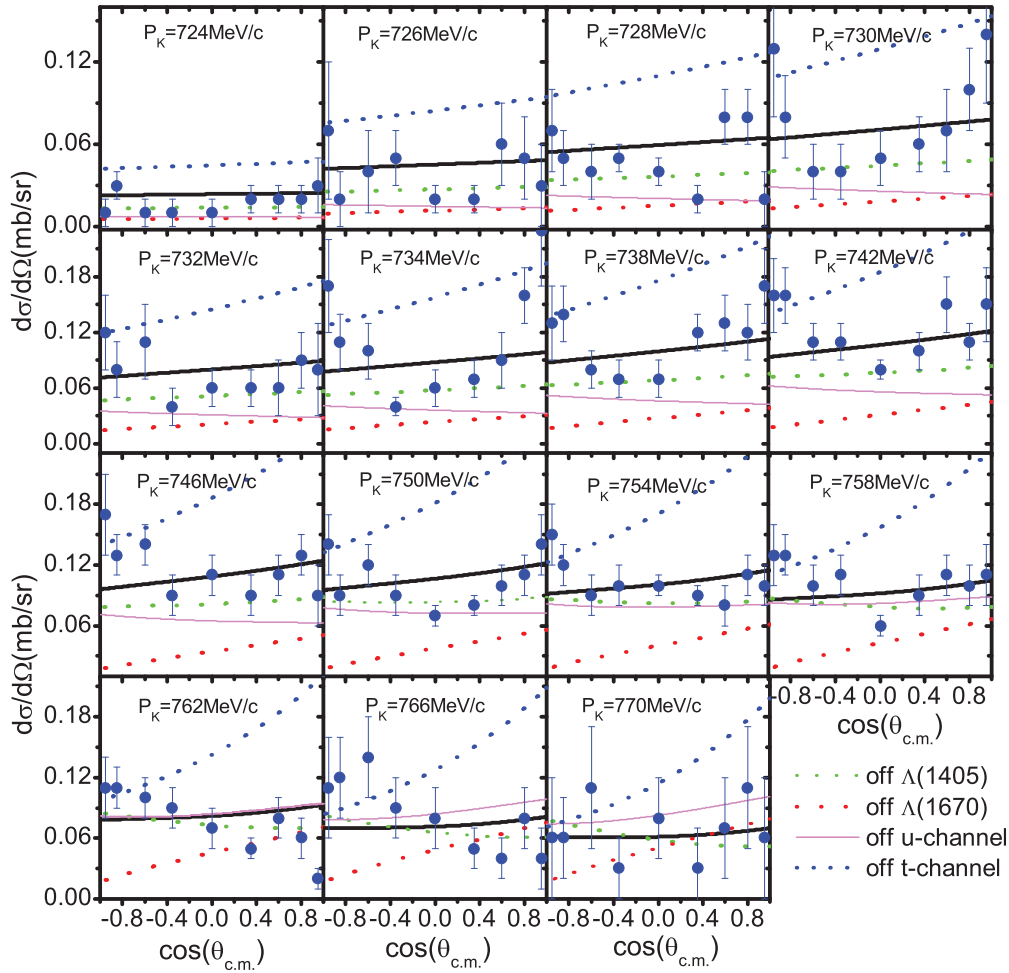
FIG. 2. (Color online) Differential cross sections of the $K^- p \rightarrow \eta \Lambda$ compared with the data from Ref. [57]. The bold solid curves are for the full model calculations. The results by switching off the contributions from $\Lambda(1405)S_{01}$, $\Lambda(1670)S_{01}$, and u- and t-channel backgrounds are indicated explicitly by the legend in the figures.

of $\Lambda(1405)S_{01}$ obtained from the $K^- p \rightarrow \Lambda \eta$ process might not be reliable enough. No obvious evidence from the D-wave states, $\Lambda(1520)D_{03}$ and $\Lambda(1690)D_{03}$, is found in the reaction.

D. Configuration mixing and strong couplings

To further understand the strength parameters C_R in the $K^- p \rightarrow \Lambda \eta$ reaction and explain the strong coupling properties of the Λ resonances extracted from the $\bar{K}N$ scattering, e.g., the weak coupling of $\Lambda(1670)S_{01}$ to $\bar{K}N$ and strong coupling of $\Lambda(1670)S_{01}$ to $\eta \Lambda$, in this section we study the configuration mixing effects in the low-lying negative Λ resonances.

1. Configuration mixing and strong decays

If there is configuration mixing in several resonances with the same J^P values, their strong coupling properties might be very different from the pure states classified in the constituent quark model. Here, we study the strong decays of low-lying negative Λ resonances and test whether the configuration mixing can explain the strong couplings of these resonances.

In this work, the strong decays of the Λ resonances also studied with the chiral quark model. This approach has been

successfully used to study the strong decays of charmed baryons, Ξ baryons, and heavy-light mesons [73–76]. The details of how to describe the strong decays of the baryon resonances in the chiral quark model can be found in Ref. [76].

As we know, $\Sigma(1385)$ is a well-estimated strangeness-1 hyperon state. According to the classification of the quark model, it is assigned to the pure $|56,^4 10, 0, 0, \frac{3}{2}^+\rangle$ representation. In this work, the measured width of $\Sigma^0(1385)$ as an input (i.e., $\Gamma = 36$ MeV [1]) is used to determine the overall parameter $\delta(= 0.654)$ in the decay amplitudes. With this determined parameter, we can calculate the strong decays of the other strangeness-1 hyperon states.

a. S-wave states. First, we study the strong decay properties of the S-wave states $\Lambda(1405)S_{01}$, $\Lambda(1670)S_{01}$, and $\Lambda(1800)S_{01}$. If they are pure states, according to the classification of the constituent quark model, they should be assigned to the $|70,^2 1, 1, 1, \frac{1}{2}^-\rangle$, $|70,^2 8, 1, 1, \frac{1}{2}^-\rangle$, and $|70,^4 8, 1, 1, \frac{1}{2}^-\rangle$, respectively [76].

Considering $\Lambda(1670)S_{01}$ as the pure state $|70,^2 8, 1, 1, \frac{1}{2}^-\rangle$, we calculate its strong decay properties, which are listed in Table V. From the table, we see that the total decay width in theory ($\Gamma_{\text{total}}^{\text{th}} = 123.4$ MeV) is much larger than that obtained

TABLE V. The predicted total and partial decay widths (MeV) and partial decay width ratios of $\Lambda(1670)S_{01}$ as a pure state of $|70,^2 8, 1, 1, \frac{1}{2}^-\rangle$. Γ^{th} denotes our prediction, while Γ^{exp} denotes the data from PDG [1].

Channel	Γ_i^{th}	Γ_{total}^{th}	Γ_{total}^{exp}	$\frac{\Gamma_i}{\Gamma_{total}}|_{th}$	$\frac{\Gamma_i}{\Gamma_{total}}|_{exp}$
$\Sigma\pi$	15.4	123.2	25 to 50 ($\approx$ 35)	0.12	0.25–0.55
NK	103.1			0.84	0.20–0.30
$\Lambda\eta$	0.001			0.00	0.10–0.25
$\Sigma(1385)\pi$	4.7			0.04	$\cdots$

from experiments ($\Gamma_{total}^{exp} \simeq 35$ MeV). Meanwhile, according to our calculation, the branching ratio of the $\Lambda\eta$ channel is too small, while the branching ratio of the $N\bar{K}$ channel is too large to compare with the data. Thus, as a pure state, the $\Lambda(1670)S_{01}$ strong decays cannot be described at all.

It should be remarked that several different representations with the same J^P numbers might be coupled together via some kind of interactions [3–5,11]. Thus, $\Lambda(1670)S_{01}$ may be a mixed state between three different representations $|70,^2 1, 1, 1\rangle$, $|70,^2 8, 1, 1\rangle$, and $|70,^4 8, 1, 1\rangle$, with $J^P = 1/2^-$. Based on the standard Cabibbo-Kobayashi-Maskawa (CKM) matrix method, the physical states might be expressed as

$$\begin{pmatrix} |\Lambda(1800)\frac{1}{2}^-\rangle \\ |\Lambda(1670)\frac{1}{2}^-\rangle \\ |\Lambda(1405)\frac{1}{2}^-\rangle \end{pmatrix} = U \begin{pmatrix} |70,^2 1\rangle \\ |70,^2 8\rangle \\ |70,^4 8\rangle \end{pmatrix}, \qquad (20)$$

with

$$U = \begin{pmatrix} c_{12}c_{13} & s_{12}c_{13} & s_{13} \\ -s_{12}c_{23} - c_{12}s_{23}s_{13} & c_{12}c_{23} - s_{12}s_{23}s_{13} & s_{23}c_{13} \\ s_{12}s_{23} - c_{12}c_{23}s_{13} & -c_{12}s_{23} - s_{12}c_{23}s_{13} & c_{23}c_{13} \end{pmatrix}, \qquad (21)$$

where $c_{ij} \equiv \cos\theta_{ij}$ and $s_{ij} \equiv \sin\theta_{ij}$. θ_{ij} stands for the mixing angles, which could be determined by fitting the strong decay data of $\Lambda(1670)S_{01}$.

By fitting the experiment data from PDG [1], we have obtained that $\theta_{12} \simeq 75°$, $\theta_{13} \simeq 50°$, and $\theta_{23} \simeq 125°$. With these mixing angles, the strong decay properties of $\Lambda(1670)S_{01}$ can be reasonably described. The theoretical results compared with the data are listed in Table VI. From the table, it is seen that with the configuration mixing the $\Lambda\eta$ branching ratio is enhanced obviously, while the $N\bar{K}$ branching ratio is suppressed, which can naturally explain the weak coupling of $\Lambda(1670)S_{01}$ to $\bar{K}N$

TABLE VI. The predicted total and partial decay widths (MeV) and partial decay width ratios of $\Lambda(1670)S_{01}$ as a mixed state compared with the experimental data from PDG [1].

Channel	Γ_i^{th}	Γ_{total}^{th}	Γ_{total}^{exp}	$\frac{\Gamma_i}{\Gamma_{total}}|_{th}$	$\frac{\Gamma_i}{\Gamma_{total}}|_{exp}$
$\Sigma\pi$	11.8	47.8	25 to 50 ($\approx$35)	0.25	0.25–0.55
NK	13.6			0.29	0.20–0.30
$\Lambda\eta$	21.3			0.44	0.10–0.25
$\Sigma(1385)\pi$	1.1			0.02	$\cdots$

and strong coupling of $\Lambda(1670)S_{01}$ to $\eta\Lambda$ needed in the $\bar{K}N$ reactions. It should be mentioned that Oset *et al.* found that $\Lambda(1670)S_{01}$ has a large coupling to $K\Xi$ channel when they analyzed the low-energy $\bar{K}N$ scattering [25]. Considering the configuration mixing effects, we indeed find that the coupling of $\Lambda(1670)S_{01}$ to $K\Xi$ channel is enhanced significantly, which is about two times larger that derived from the symmetry quark model. The coupling ratios obtained for the $\Lambda(1670)S_{01}$ are

$$|g_{\bar{K}N}|^2 : |g_{K\Xi}|^2 : |g_{\eta\Lambda}|^2 \simeq 0.7 : 8.4 : 1.0, \qquad (22)$$

which are compatible with the predictions in Ref. [25].

According to the determined mixing angles, Eq. (20) can be explicitly expressed as

$$\begin{pmatrix} |\Lambda(1800)\frac{1}{2}^-\rangle \\ |\Lambda(1670)\frac{1}{2}^-\rangle \\ |\Lambda(1405)\frac{1}{2}^-\rangle \end{pmatrix} = \begin{pmatrix} 0.17 & 0.62 & 0.77 \\ 0.39 & -0.76 & 0.53 \\ 0.90 & 0.21 & -0.37 \end{pmatrix} \begin{pmatrix} |70,^2 1\rangle \\ |70,^2 8\rangle \\ |70,^4 8\rangle \end{pmatrix}, \qquad (23)$$

where we find that the main component of $\Lambda(1670)S_{01}$ is $|70,^2 8\rangle (\sim 58\%)$. Meanwhile, the $|70,^2 1\rangle$ and $|70,^4 8\rangle$ components also have a sizable proportion, which are $\sim 15\%$ and $\sim 28\%$, respectively. $\Lambda(1405)S_{01}$ is dominated by the $|70,^2 1\rangle (\sim 81\%)$, while it contains significant octet components of $|70,^2 8\rangle (\sim 4\%)$ and $|70,^4 8\rangle (\sim 14\%)$. $\Lambda(1800)S_{01}$ is dominated by both the $|70,^4 8\rangle (\sim 59\%)$ and $|70,^2 8\rangle (\sim 38\%)$ components.

With these mixing schemes, we have calculated the strong decay properties of $\Lambda(1405)S_{01}$ and $\Lambda(1800)S_{01}$. The calculated decay width of $\Lambda(1405)S_{01}$ is $\Gamma \simeq 53$ MeV, which is in good agreement with the data ($\Gamma = 50 \pm 2$ MeV).

Considering the uncertainties in the mass of $\Lambda(1800)S_{01}$, we vary its mass from 1700 to 1870 MeV. The predicted strong decay properties of $\Lambda(1800)S_{01}$ have been shown in Fig. 3. From the figure, we can see that the strong decays of $\Lambda(1800)S_{01}$ are dominated by the $\bar{K}N$, $\eta\Lambda$, and $\Sigma\pi$ decay modes, while the decay channel $\Sigma(1385)\pi$ also has a significant contribution to the strong decays of $\Lambda(1800)S_{01}$. It is found that our predicted strong decay properties of $\Lambda(1800)S_{01}$ are compatible with the data of ALSTON (see Table VII) [77]. About $\Lambda(1800)S_{01}$, more measurements are needed in the experiments.
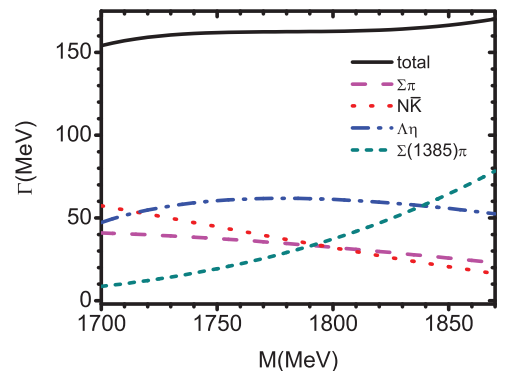
FIG. 3. (Color online) The strong decay properties of $\Lambda(1800)S_{01}$, which is taken as a mixed state in Eq. (20).

TABLE VII. The predicted total and partial decay widths (MeV) of $\Lambda(1800)S_{01}$ compared with the experimental data from ALSTON [77]. We set the mass of $\Lambda(1800)S_{01}$ as $M = 1725$ MeV, which is the observed value from ALSTON.

Channel	$N\bar{K}$	$\Sigma\pi$	$\Lambda\eta$	$\Sigma(1385)\pi$
Γ_i^{th}	51.1	39.5	56.1	13.2
Γ_i^{exp}	52 ± 9	$\cdots$	$\cdots$	$\cdots$

As a whole, the configuration mixing is needed to understand the strong decay properties of the S-wave resonances $\Lambda(1405)S_{01}$, $\Lambda(1670)S_{01}$, and $\Lambda(1800)S_{01}$.

b. D-wave states. Then we further study whether the configuration mixing is necessary to explain the strong decays of the well-established D-wave resonances $\Lambda(1520)D_{03}$ and $\Lambda(1690)D_{03}$. If $\Lambda(1520)D_{03}$ and $\Lambda(1690)D_{03}$ are pure states, they should be classified as the $|70,^2 1, 1, 1, \frac{3}{2}^-\rangle$ and $|70,^4 8, 1, 1, \frac{3}{2}^-\rangle$ configurations, respectively, in the constituent quark model.

First, we study the decay properties of $\Lambda(1520)D_{03}$ and $\Lambda(1690)D_{03}$ as pure states. The predictions compared with the data are listed in Tables VIII and IX, respectively.

From Table VIII, we find that as a pure state the strong decay coupling of $\Lambda(1520)D_{03}$ to $\Sigma\pi$ is overestimated. However, the strong coupling of $\Lambda(1520)D_{03}$ to $N\bar{K}$ is underestimated, which is also found in the $\bar{K}N$ scattering [56].

While considering $\Lambda(1690)D_{03}$ as a pure state $|70,^4 8, 1, 1, \frac{3}{2}^-\rangle$, from Table IX we find that the theoretical predictions are inconsistent with the experimental observations. The predicted total decay width is much larger than that obtained from experiments. In addition, the partial decay width ratio for $\Sigma\pi$ is too small, while that for $N\bar{K}$ is too large to compare with the data. Thus, as pure states, the strong decay properties of $\Lambda(1520)D_{03}$ and $\Lambda(1690)D_{03}$ cannot be understood reasonably.

For these reasons, it is natural for us to take $\Lambda(1520)$ and $\Lambda(1690)$ as two mixing states among $|70,^2 1, 1, 1, \frac{3}{2}^-\rangle$, $|70,^2 8, 1, 1, \frac{3}{2}^-\rangle$, and $|70,^4 8, 1, 1, \frac{3}{2}^-\rangle$. By the using of the CKM matrix method again, and fitting the strong decay data of $\Lambda(1690)$, we obtain

$$\begin{pmatrix} |\Lambda(1520)\frac{3}{2}^-\rangle \\ |\Lambda(1690)\frac{3}{2}^-\rangle \\ |\Lambda\frac{3}{2}^-\rangle_3 \end{pmatrix} = \begin{pmatrix} 0.94 & 0.34 & 0.09 \\ 0.31 & -0.92 & 0.26 \\ 0.17 & -0.21 & -0.96 \end{pmatrix} \begin{pmatrix} |70,^2 1\rangle \\ |70,^2 8\rangle \\ |70,^4 8\rangle \end{pmatrix}.$$

(24)

TABLE VIII. The predicted total and partial decay widths (MeV) and partial decay width ratios of $\Lambda(1520)D_{03}$ as a pure state $|70,^2 1, 1, 1, \frac{3}{2}^-\rangle$ compared with the experimental data from PDG [1].

Channel	Γ_i^{th}	Γ_{total}^{th}	Γ_{total}^{exp}	$\frac{\Gamma_i}{\Gamma_{total}}|_{th}$	$\frac{\Gamma_i}{\Gamma_{total}}|_{exp}$
$\Sigma\pi$	10.7	14.5	15.6 ± 1.0	0.74	0.42 ± 0.01
NK	3.8			0.26	0.45 ± 0.01

TABLE IX. The predicted total and partial decay widths (MeV) and partial decay width ratios of $\Lambda(1690)D_{03}$ as a pure state of $|70,^2 8, 1, 1, \frac{3}{2}^-\rangle$ compared with the experiment data from PDG [1].

Channel	Γ_i^{th}	Γ_{total}^{th}	Γ_{total}^{exp}	$\frac{\Gamma_i}{\Gamma_{total}}|_{th}$	$\frac{\Gamma_i}{\Gamma_{total}}|_{exp}$
$\Sigma\pi$	9.7	117.2	50–70 (≈ 60)	0.08	0.20–0.40
NK	58.3			0.50	0.20–0.30
$\Lambda\eta$	0.001			0.00	$\cdots$
$\Sigma(1385)\pi$	49.1			0.42	$\cdots$

From Eq. (24), it is seen that $\Lambda(1690)$ has sizable components of $|70,^2 1\rangle$ ($\sim 9\%$) and $|70,^4 8\rangle$ ($\sim 7\%$), except for the main component $|70,^2 8\rangle$ ($\sim 85\%$). The predicted strong decay properties of $\Lambda(1690)D_{03}$ compared with the data are listed in Table X, where we find that with the configuration mixing effects, the strong decays of $\Lambda(1690)D_{03}$ can be well described. It should be emphasized that $\Lambda(1690)$ has a very weak coupling to $\Lambda\eta$, although it has been enhanced significantly by considering the configuration mixing effects, which gives an explanation as to why the contribution of $\Lambda(1690)D_{03}$ to the reaction $K^- p \to \Lambda\eta$ is tiny even though $\Lambda(1690)D_{03}$ has a large C_R factor.

Furthermore, with the mixing scheme determined in Eq. (24), we study the strong decay of $\Lambda(1520)D_{03}$. The predicted results compared with the data are listed in Table XI, where we find both the total decay width and the partial decay width ratios are in good agreement with the data. The $N\bar{K}$ branching ratio is about a factor 2 larger than that derived in the SU(6) $\otimes$ O(3) limit, which is consistent with our previous analysis of the $\bar{K}N$ scattering in Ref. [56]. From Eq. (24), we can see that the main component of $\Lambda(1520)D_{03}$ is still the $|70,^2 1\rangle$ configuration ($\sim 88\%$), while it contains significant octet component of $|70,^2 8\rangle$ ($\sim 12\%$).

Finally, we give our predictions of the third D-wave resonance $|\Lambda\frac{3}{2}^-\rangle_3$, which is still not established in experiment. According to the quark model prediction, its mass is around 1800 MeV [3–5,11]. Varying its mass from 1700 to 1900 MeV, we calculate the strong decays of $|\Lambda\frac{3}{2}^-\rangle_3$. Our predictions are shown in Fig. 4. It is found that the strong decays of $|\Lambda\frac{3}{2}^-\rangle_3$ are dominated by $\Sigma(1385)\pi$ and $\Sigma\pi$, while the $N\bar{K}$ and $\Lambda\eta$ branching ratios are negligibly small. Thus, we suggest that our experimental colleagues find this missing D-wave state in the $\Sigma(1385)\pi$ and $\Sigma\pi$ channels.

In short, the configuration mixing is also needed to understand the strong decay properties of the D-wave resonances $\Lambda(1520)D_{03}$ and $\Lambda(1690)D_{03}$.

TABLE X. The predicted total and partial decay widths (MeV) and partial decay width ratios of $\Lambda(1690)$ as a mixed state compared with the experimental data from PDG [1].

Channel	Γ_i^{th}	Γ_{total}^{th}	Γ_{total}^{exp}	$\frac{\Gamma_i}{\Gamma_{total}}|_{th}$	$\frac{\Gamma_i}{\Gamma_{total}}|_{exp}$
$\Sigma\pi$	27.5	70.6	50–70 (≈ 60)	0.39	0.20–0.40
NK	21.4			0.30	0.20–0.30
$\Lambda\eta$	0.01			0.00	$\cdots$
$\Sigma(1385)\pi$	21.6			0.30	$\cdots$

TABLE XI. The predicted total and partial decay widths (MeV) and partial decay width ratios of $\Lambda(1520)$ as a mixed state compared with the experimental data from PDG [1].

Channel	Γ_i^{th}	$\Gamma_{\text{total}}^{\text{th}}$	$\Gamma_{\text{total}}^{\text{exp}}$	$\frac{\Gamma_i}{\Gamma_{\text{total}}}\vert_{\text{th}}$	$\frac{\Gamma_i}{\Gamma_{\text{total}}}\vert_{\text{exp}}$
$\Sigma\pi$	7.0	13.5	15.6–1.0	0.52	0.42 ± 0.01
NK	6.2			0.46	0.45 ± 0.01
$\Sigma(1385)\pi$	0.3			0.02	$\cdots$

2. Interpretation of C_R with configuration mixing

If the configuration mixing effects are included, the single-resonance-excitation amplitude given in Eq. (7) should be rewritten as

$$\mathcal{O}(n, l, J) = \sum_R g_R' \mathcal{O}(n, l, J) \equiv \sum_R C_R g_R \mathcal{O}(n, l, J), \quad (25)$$

where g_R' (g_R) stands for the relative strength of a single-resonance with (without) configuration mixing effects in the partial amplitude $\mathcal{O}(n, l, J)$. The C_R parameters can be derived by

$$C_R = \frac{g_R'}{g_R}. \quad (26)$$

In the following work, we study the C_R parameters of the important resonances $\Lambda(1405)S_{01}$, $\Lambda(1670)S_{01}$, $\Lambda(1520)D_{03}$, and $\Lambda(1690)D_{03}$ for the $K^- p \to \eta\Lambda$ process.

Taking $\Lambda(1405)S_{01}$, $\Lambda(1670)S_{01}$, $\Lambda(1520)D_{03}$, and $\Lambda(1690)D_{03}$ as pure states in the constituent quark model, we can derive the couplings of the transition amplitudes for these resonances, which are given by

$$R_{\Lambda(1405)} = -\frac{\sqrt{3}}{108}(\sqrt{2}\sin\phi_P + \cos\phi_P), \quad (27)$$

$$R_{\Lambda(1670)} = -\frac{\sqrt{3}}{108}(\sqrt{2}\sin\phi_P - \cos\phi_P), \quad (28)$$

$$R_{\Lambda(1520)} = -\frac{\sqrt{3}}{54}(\sqrt{2}\sin\phi_P + \cos\phi_P), \quad (29)$$

$$R_{\Lambda(1690)} = -\frac{\sqrt{3}}{54}(\sqrt{2}\sin\phi_P - \cos\phi_P), \quad (30)$$
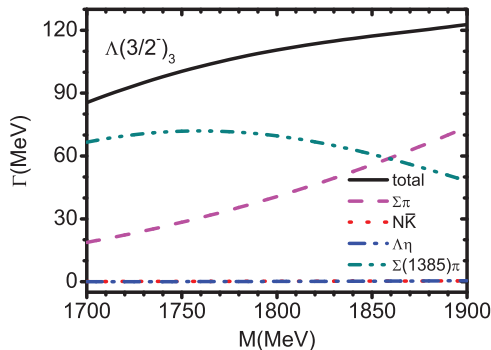
FIG. 4. (Color online) The strong decay properties of $|\Lambda\frac{3}{2}^-\rangle_3$ as a counterpart of $\Lambda(1690)$.

where the ϕ_P is the η-η' mixing angle. Then the g_R parameters for these states can be obtained by

$$g_{\Lambda(1405)\text{or}\Lambda(1670)} = \frac{R_{\Lambda(1405)}\text{or}R_{\Lambda(1670)}}{R_{\Lambda(1405)} + R_{\Lambda(1670)}}, \quad (31)$$

$$g_{\Lambda(1520)\text{or}\Lambda(1690)} = \frac{R_{\Lambda(1520)}\text{or}R_{\Lambda(1690)}}{R_{\Lambda(1520)} + R_{\Lambda(1690)}}. \quad (32)$$

Considering the configuration mixing effects, the wave functions of the S- and D-wave states $\Lambda(1405)S_{01}$, $\Lambda(1670)S_{01}$, $\Lambda(1520)D_{03}$, and $\Lambda(1690)D_{03}$ can be generally written as

$$|\Lambda(1405)\rangle = a_1|70,^2 1\rangle_S + b_1|70,^2 8\rangle_S + c_1|70,^4 8\rangle_S, \quad (33)$$

$$|\Lambda(1670)\rangle = a_2|70,^2 1\rangle_S + b_2|70,^2 8\rangle_S + c_2|70,^4 8\rangle_S, \quad (34)$$

$$|\Lambda(1520)\rangle = a_3|70,^2 1\rangle_D + b_3|70,^2 8\rangle_D + c_3|70,^4 8\rangle_D, \quad (35)$$

$$|\Lambda(1690)\rangle = a_4|70,^2 1\rangle_D + b_4|70,^2 8\rangle_D + c_4|70,^4 8\rangle_D, \quad (36)$$

where a_i, b_i, and c_i ($i = 1, 2, 3, 4$) have been determined in Eqs. (23) and (24). Then we can derive the couplings of the transition amplitudes for these mixed states; they are

$$R'_{\Lambda(1405)} = -\frac{\sqrt{3}}{108}(\sqrt{2}\sin\phi_P + \cos\phi_P)(a_1^2 + a_1 b_1)$$
$$- \frac{\sqrt{3}}{108}(\sqrt{2}\sin\phi_P - \cos\phi_P)(b_1^2 + a_1 b_1), \quad (37)$$

$$R'_{\Lambda(1670)} = -\frac{\sqrt{3}}{108}(\sqrt{2}\sin\phi_P + \cos\phi_P)(a_2^2 + a_2 b_2)$$
$$- \frac{\sqrt{3}}{108}(\sqrt{2}\sin\phi_P - \cos\phi_P)(b_2^2 + a_2 b_2), \quad (38)$$

$$R'_{\Lambda(1520)} = -\frac{\sqrt{3}}{54}(\sqrt{2}\sin\phi_P + \cos\phi_P)(a_3^2 + a_3 b_3)$$
$$- \frac{\sqrt{3}}{54}(\sqrt{2}\sin\phi_P - \cos\phi_P)(b_3^2 + a_3 b_3), \quad (39)$$

$$R'_{\Lambda(1690)} = -\frac{\sqrt{3}}{54}(\sqrt{2}\sin\phi_P + \cos\phi_P)(a_4^2 + a_4 b_4)$$
$$- \frac{\sqrt{3}}{54}(\sqrt{2}\sin\phi_P - \cos\phi_P)(b_4^2 + a_4 b_4). \quad (40)$$

Finally, we obtain the relative strength parameters g_R' for these mixed states:

$$g'_{\Lambda(1405)\text{or}\Lambda(1670)} = \frac{R'_{\Lambda(1405)}\text{or}R'_{\Lambda(1670)}}{R'_{\Lambda(1405)} + R'_{\Lambda(1670)}}, \quad (41)$$

$$g'_{\Lambda(1520)\text{or}\Lambda(1690)} = \frac{R'_{\Lambda(1520)}\text{or}R'_{\Lambda(1690)}}{R'_{\Lambda(1520)} + R'_{\Lambda(1690)}}. \quad (42)$$

With these extracted g_R and g_R' parameters, the C_R parameters can be easily worked out according to Eq. (26). It is found that C_R is a function of the η-η' mixing angle ϕ_P, which might be in the range $\phi_P \simeq (30°, 47°)$ [68,69]. Considering the uncertainties of ϕ_P, we plot C_R as a function of ϕ_P in Fig. 5. From the figure, one can find that the C_R parameters for $\Lambda(1670)S_{01}$ and $\Lambda(1690)D_{03}$ are sensitive to the η-η' mixing angle ϕ_P. When taking a small η-η' mixing angle $\phi_P = 35°$, we obtain a large value $C_{\Lambda(1670)} \simeq 34$ for $\Lambda(1670)S_{01}$, which
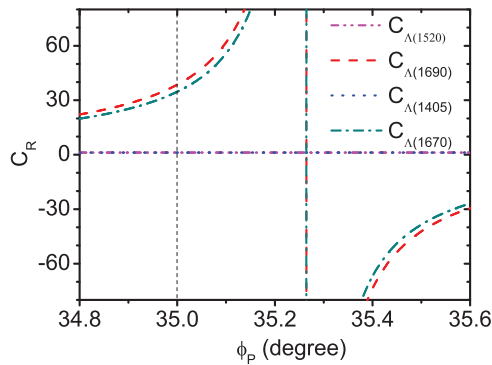
FIG. 5. (Color online) The coupling strength parameter, C_R, as a function of the η-η' mixing angle ϕ_P.

can naturally explain the large contributions of $\Lambda(1670)S_{01}$ found in the $K^- p \to \Lambda \eta$ process.

Using the determined η-η' mixing angle $\phi_P = 35°$, we also obtain a large value of $C_{\Lambda(1690)} \simeq 39$ for $\Lambda(1690)D_{03}$. It is should be mentioned that although the configuration mixing effects have largely enhanced the contribution of $\Lambda(1690)$ in the $K^- p \to \Lambda \eta$ process (about a factor of 39), the contribution of $\Lambda(1690)D_{03}$ in the reaction is still negligibly small for the very weak coupling to $\eta \Lambda$.

As a whole, the configuration mixing effects are crucial to understand the strong decay properties of the low-lying negative Λ resonances. These resonances are most likely mixed states between different configurations, which is consistent with the predictions in large N_c QCD [11]. Considering configuration mixing effects, we can reasonably explain the weak coupling of $\Lambda(1670)S_{01}$ to $\bar{K}N$ and strong coupling of $\Lambda(1670)S_{01}$ to $\eta \Lambda$ and the large strength parameter $C_{\Lambda(1670)} \simeq 34$. It should be mentioned that the hadronic dressing mechanisms might bring some additional effects to the couplings [40,70,71], which is not studied here for the limitation of our model. The contribution of $\Lambda(1690)D_{03}$ to the $K^- p \to \Lambda \eta$ process is too small to give a bowl structure in the DCS, even when we consider the configuration mixing effects in these D-wave states.

IV. SUMMARY

In this work, we have studied the low-energy reaction $K^- p \to \Lambda \eta$ with a chiral quark model approach. A reasonable description of the measurements has been achieved. It is found that $\Lambda(1670)S_{01}$ dominates the reaction around at the low-energy regions, and the t- and u-channel backgrounds also play crucial roles. Slight contributions of $\Lambda(1405)S_{01}$

are found; however, $\Lambda(1405)S_{01}$ does not obviously affect the shapes of the DCSs. No obvious roles of the D-wave states $\Lambda(1520)D_{03}$ and $\Lambda(1690)D_{03}$ are found in the reaction.

Furthermore, by the study of the $K^- p \to \Lambda \eta$ process, we have extracted the strong interaction properties of $\Lambda(1670)S_{01}$. We find that a much larger amplitude of $\Lambda(1670)S_{01}$ in the reaction is needed, which is about 34 times (i.e., $C_{S_{01}(1670)} \simeq 34$) larger than that derived from the symmetry quark model. Combing this with our previous study in Ref. [56], we conclude that $\Lambda(1670)S_{01}$ should have a much weaker coupling to $\bar{K}N$, while a much stronger coupling to $\eta \Lambda$ than that predicted in the symmetry quark model.

To understand these strong interaction properties of $\Lambda(1670)S_{01}$, we further study the strong decay properties of the low-lying negative parity Λ resonances. It is found that the configuration mixing effects are crucial to understand the strong decay properties of the low-lying negative Λ resonances. These resonances are most likely mixed states between different configurations. Considering configuration mixing effects, we can reasonably explain the strong interaction properties of $\Lambda(1670)S_{01}$ extracted from the $K^- p \to \Lambda \eta$.

The data of the $K^- p \to \Lambda \eta$ process show that there seems to be a bowl structure in the DCS in a narrow energy region near the $\eta \Lambda$ threshold, which indicates a strong D-wave contribution there. However, the contribution of $\Lambda(1690)D_{03}$ to the $K^- p \to \Lambda \eta$ process is too small to give a bowl structure in the DCS. Although with the configuration mixing effects in these D-wave states, the amplitude of $\Lambda(1690)D_{03}$ in the reaction could be enhanced a factor of $\sim$39, the contribution of $\Lambda(1690)D_{03}$ is still tiny for the very weak coupling of $\Lambda(1690)D_{03}$ to $\eta \Lambda$. Based on the bowl structures in the DCS, Liu and Xie believed there might be an exotic D-wave state $\Lambda(1669)D_{03}$ with a very narrow width of $\Gamma = 1.5$ MeV. To clarify whether there are contributions of a narrow D-wave state, more accurate measurements are needed.

As a byproduct, we also have predicted the strong decay properties of the unestablished D-wave state $|\Lambda \frac{3}{2}^-\rangle_3$. This resonance mainly decays into $\Sigma(1385)\pi$ and $\Sigma \pi$ channels. We hope the experimentalists can search this missing D-wave state in the $\Sigma(1385)\pi$ and $\Sigma \pi$ channels.

[1] J. Beringer *et al.* (Particle Data Group), Phys. Rev. D **86**, 010001 (2012).

[2] E. Klempt and J.-M. Richard, Rev. Mod. Phys. **82**, 1095 (2010).

[3] N. Isgur and G. Karl, Phys. Rev. D **18**, 4187 (1978).

[4] N. Isgur and G. Karl, Phys. Lett. B **72**, 109 (1977); Phys. Rev. D **19**, 2653 (1979); N. Isgur, *ibid*. **23**, 817(E) (1981); N. Isgur and G. Karl, *ibid*.**20**, 1191 (1979).

[5] S. Capstick and N. Isgur, Phys. Rev. D **34**, 2809 (1986).

[6] Y. Chen and B.-Q. Ma, Nucl. Phys. A **831**, 1 (2009).

[7] T. Melde, W. Plessas, and B. Sengl, Phys. Rev. D **77**, 114002 (2008).

[8] R. Bijker, F. Iachello, and A. Leviatan, Ann. Phys. **284**, 89 (2000).

[9] L. Y. Glozman, W. Plessas, K. Varga, and R. F. Wagenbrunn, Phys. Rev. D **58**, 094030 (1998).

[10] U. Loring, B. C. Metsch, and H. R. Petry, Eur. Phys. J. A **10**, 447 (2001).

[11] C. L. Schat, J. L. Goity, and N. N. Scoccola, Phys. Rev. Lett. **88**, 102002 (2002).

[12] J. L. Goity, C. L. Schat, and N. N. Scoccola, Phys. Rev. D **66**, 114014 (2002).

[13] B. J. Menadue, W. Kamleh, D. B. Leinweber, and M. S. Mahbub, Phys. Rev. Lett. **108**, 112001 (2012).

[14] G. P. Engel, C. B. Lang, and A. Schafer, Phys. Rev. D. **87**, 034502 (2013).

[15] R. Koniuk and N. Isgur, Phys. Rev. D **21**, 1868 (1980); **23**, 818(E) (1981).

[16] T. Melde, W. Plessas, and B. Sengl, Phys. Rev. C **76**, 025204 (2007).

[17] T. Melde and W. Plessas, Eur. Phys. J. A **35**, 329 (2008).

[18] C. S. An, B. Saghai, S. G. Yuan, and J. He, Phys. Rev. C **81**, 045203 (2010).

[19] T. Hyodo and D. Jido, Prog. Part. Nucl. Phys. **67**, 55 (2012).

[20] J. A. Oller, J. Prades, and M. Verbeni, Phys. Rev. Lett. **95**, 172502 (2005).

[21] L. Roca, S. Sarkar, V. K. Magas, and E. Oset, Phys. Rev. C **73**, 045208 (2006).

[22] B. Borasoy, R. Nissler, and W. Weise, Eur. Phys. J. A **25**, 79 (2005).

[23] T. Hyodo, S. i. Nam, D. Jido, and A. Hosaka, Prog. Theor. Phys. **112**, 73 (2004).

[24] D. Jido, J. A. Oller, E. Oset, A. Ramos, and U. G. Meissner, Nucl. Phys. A **725**, 181 (2003).

[25] E. Oset, A. Ramos, and C. Bennhold, Phys. Lett. B **527**, 99 (2002); **530**, 260(E) (2002).

[26] C. Garcia-Recio, J. Nieves, E. R. Arriola, and M. J. Vicente Vacas, Phys. Rev. D **67**, 076009 (2003).

[27] J. A. Oller and U. G. Meissner, Phys. Lett. B **500**, 263 (2001).

[28] E. Oset and A. Ramos, Nucl. Phys. A **635**, 99 (1998).

[29] J. A. Oller, Eur. Phys. J. A **28**, 63 (2006).

[30] J. A. Oller, J. Prades, and M. Verbeni, Eur. Phys. J. A **31**, 527 (2007).

[31] B. Borasoy, U. G. Meissner, and R. Nissler, Phys. Rev. C **74**, 055201 (2006).

[32] L. Roca, T. Hyodo, and D. Jido, Nucl. Phys. A **809**, 65 (2008).

[33] M. Doring, D. Jido, and E. Oset, Eur. Phys. J. A **45**, 319 (2010).

[34] M. Doring, J. Haidenbauer, U.-G. Meissner, and A. Rusetsky, Eur. Phys. J. A **47**, 163 (2011).

[35] Antonio O. Bouzasa, Eur. Phys. J. A **37**, 201 (2008).

[36] A. D. Martin, N. M. Queen, and G. Violini, Nucl. Phys. B **10**, 481 (1969).

[37] D. M. Manley *et al.*, Phys. Rev. Lett. **88**, 012002 (2001).

[38] M. F. M. Lutz and E. E. Kolomeitsev, Nucl. Phys. A **700**, 193 (2002).

[39] R. Buttgen, K. Holinde, and J. Speth, Phys. Lett. B **163**, 305 (1985).

[40] A. Mueller-Groeling, K. Holinde, and J. Speth, Nucl. Phys. A **513**, 557 (1990).

[41] T. Hamaie, M. Arima, and K. Masutani, Nucl. Phys. A **591**, 675 (1995).

[42] X. H. Zhong and Q. Zhao, Phys. Rev. C **79**, 045202 (2009).

[43] A. D. Martin, Nucl. Phys. B **179**, 33 (1981).

[44] P. M. Gensini, R. Hurtado, and G. Violini, PiN Newslett. **13**, 291 (1997).

[45] Z.-H. Guo and J. A. Oller, Phys. Rev. C **87**, 035202 (2013).

[46] H. Zhang, J. Tulpan, M. Shrestha, and D. M. Manley, Phys. Rev. C **88**, 035204 (2013).

[47] H. Zhang, J. Tulpan, M. Shrestha, and D. M. Manley, Phys. Rev. C **88**, 035205 (2013).

[48] L. S. Geng and E. Oset, Eur. Phys. J. A **34**, 405 (2007).

[49] L. S. Geng, E. Oset, and M. Doring, Eur. Phys. J. A **32**, 201 (2007).

[50] L. S. Geng, E. Oset, and B. S. Zou, Eur. Phys. J. A **38**, 239 (2008).

[51] B.-C. Liu and J.-J. Xie, Phys. Rev. C **86**, 055202 (2012).

[52] B.-C. Liu and J.-J. Xie, Phys. Rev. C **85**, 038201 (2012).

[53] J.-J. Xie, B.-C. Liu, and C.-S. An, Phys. Rev. C **88**, 015203 (2013).

[54] C. Garcia-Recio, M. F. M. Lutz, and J. Nieves, Phys. Lett. B **582**, 49 (2004).

[55] B. S. Zou, eConf C **070910**, 112 (2007); Chin. Phys. C **33**, 1113 (2009).

[56] X.-H. Zhong and Q. Zhao, Phys. Rev. C **88**, 015208 (2013).

[57] A. Starostin *et al.* (Crystal Ball Collaboration), Phys. Rev. C **64**, 055205 (2001).

[58] Z. P. Li, Phys. Rev. D **48**, 3070 (1993); **50**, 5639 (1994); **52**, 4961 (1995); Phys. Rev. C **52**, 1648 (1995).

[59] Z. P. Li, H. X. Ye, and M. H. Lu, Phys. Rev. C **56**, 1099 (1997).

[60] Q. Zhao, J. S. Al-Khalili, and C. Bennhold, Phys. Rev. C **64**, 052201(R) (2001).

[61] Q. Zhao, B. Saghai, and Z. P. Li, J. Phys. G **28**, 1293 (2002).

[62] Q. Zhao, Z. P. Li, and C. Bennhold, Phys. Rev. C **58**, 2393 (1998); Phys. Lett. B **436**, 42 (1998).

[63] J. He, B. Saghai, and Z. Li, Phys. Rev. C **78**, 035204 (2008).

[64] B. Saghai and Z. P. Li, Eur. Phys. J. A **11**, 217 (2001).

[65] Q. Zhao, J. S. Al-Khalili, Z. P. Li, and R. L. Workman, Phys. Rev. C **65**, 065204 (2002).

[66] X.-H. Zhong and Q. Zhao, Phys. Rev. C **84**, 065204 (2011); **84**, 045207 (2011).

[67] X. H. Zhong, Q. Zhao, J. He, and B. Saghai, Phys. Rev. C **76**, 065205 (2007).

[68] C. Di Donato, G. Ricciardi and I. I. Bigi, Phys. Rev. D **85**, 013016 (2012).

[69] H.-W. Ke, X.-Q. Li, and Z.-T. Wei, Eur. Phys. J. C **69**, 133 (2010).

[70] M. Doring, C. Hanhart, F. Huang, S. Krewald, and U.-G. Meissner, Phys. Lett. B **681**, 26 (2009).

[71] M. Doring, C. Hanhart, F. Huang, S. Krewald, and U.-G. Meissner, Nucl. Phys. A **829**, 170 (2009).

[72] Q. Zhao and F. E. Close, Phys. Rev. D **74**, 094014 (2006).

[73] X. H. Zhong and Q. Zhao, Phys. Rev. D **77**, 074008 (2008); **78**, 014029 (2008); **81**, 014031 (2010).

[74] X.-H. Zhong, Phys. Rev. D **82**, 114014 (2010).

[75] L.-H. Liu, L.-Y. Xiao, and X.-H. Zhong, Phys. Rev. D **86**, 034024 (2012).

[76] L.-Y. Xiao and X.-H. Zhong, Phys. Rev. D **87**, 094002 (2013).

[77] M. Alston-Garnjost, R. W. Kenney, D. L. Pollard, R. R. Ross, R. D. Tripp, H. Nicholson, and M. Ferro-Luzzi, Phys. Rev. D **18**, 182 (1978).